

MRI images de-noising based in Dual-Tree complex Wavelet and Bayesian MAP Estimator

R.Mavudila¹, Lh.Masmoudi², M.Cherkaoui³, N.Hassanain⁴

(physics department ,LETS Laboratory /Faculty of Science/, Mohammed V University/Morocco)

(physics department ,LETS Laboratory /Faculty of Science/, Mohammed V University/Morocco)

(Faculty of medicine and pharmacy/, SIDI Mohammed Ben Abdellah University/CHU CheikZaid/ Morocco)

(physics department ,LETS Laboratory /Faculty of Science/, Mohammed V University/Morocco)

ABSTRACT: MRI images are often subject to noise (artifacts). We evaluated the performance of DT-CWT combined to Bayesian MAP Estimator to restore those images.

We chose the images from two of four sequences commonly used in coronal and axial MRI with and without contrast agent. The image with contrast agent was used as a reference, and the image without where we added artificially noise was subjected to de-noising by forward Dual-Tree Wavelet Transform (DT-CWT) combined to Bayesian MAP estimator. A test was submitted to radiologists for an assessment of the de-noised images to compare the proposed algorithm to other effective techniques from the recent literature using MRI images. Our approach contributed effectively to the MRI images de-noising, with better results. In general, wavelets and Bayesian estimator contributed effectively to the de-noising process and to other image processing methods, but ranging from classic to complex wavelet transforms, the results gradually improved.

Keywords: Bayesian MAP, Complex Wavelet, Dual-Tree Wavelet transform, Image de-noising, MRI images.

I. INTRODUCTION

The digital representation of images has been controversial since the early days of computing. Because images are innately strong in semantic content, they quickly became a frequently used communication medium.

Images are also an essential tool in the fields of biomedicine and satellite and astronomical imaging, among others.

Medical imaging has revolutionized medicine by allowing doctors to retrieve potentially vital information from inside the human body in a noninvasive manner, as is the case for MRI that we focused on in our study. In Magnetic resonance, the practical limits of the acquisition time impose a trade-off between the SNR and the image resolution [1,2,3]

In this paper, we address the problem of MRI images de-noising.

In MRI, acquisition protocols lead to image quality loss, particularly with contrast, because of the presence of artifacts that make their interpretation difficult [4,6] and this noise in the MRI image magnitude is Rician [5], having a signal dependent mean.

Many challengers have been made to remove this noise using wavelet transform as described briefly.

WiemFourati and Mohammed Salim. B (2007) proposed a de-noising method based on the statistical dependency of wavelet coefficients and on the application of an adaptive Bivshrink type MAP filter (Maximum Posterior Estimator) [7].

From a method described by Donoho, Alendru in [9]. I and al. have proposed a de-noising scheme based on a wavelet transform named discrete wavelet transform with enriched diversity (TODDE), combining several families of wavelets and various estimators in Bishrink occurrence to eliminate the noise (speckle) in the images, which also applies to ultrasound images [8].

Previously proposed wavelet domain filtering techniques were based on different thresholding schemes where the coefficient selection was based on inter-scale correlations [5,11,12],

It was noted that due to the signal dependent mean of the Rician noise, both wavelet and scaling coefficients of a noisy MRI image are biased estimates of their noise-free counterparts [5].

In addition it was shown that one can efficiently overcome this problem by filtering the square of the MRI image in wavelet domain.

In the wavelet domain, the Discrete Wavelet Transform (DWT) has a limits and major disadvantages that undermines its application for some image processing as; lack of shift invariance, poor directional selectivity for diagonal features and other.. [10].

A comprehensive review of previous work shows the performance of these tools for image de-noising, although performance suffers from the classical wavelet limits of certain processing treatments, especially for the specificity of medical images.

The objective of this study was to use the DT-CWT and Bayesian approach that is based on a Symmetric Normal Inverse Gaussian (SNIG) [13] this model is useful for smoothing disease relative risk estimates.

The object is to de-noise images, in which the use of contrast agents could have affected the distinct visualization of healthy and pathological tissues.

The images with contrast agent were used as controls, and the images without contrast were used as images to restore, with the aim of obtaining images similar to the ones with contrast agent. In spite of existing mathematical methods, such as PSNR, correlation, and so forth, we used a human visual system (HSV), consisting of a blind test based on specific and precise criteria such as quality, sharpness, and the clinicians' ability to arrive at a correct diagnosis.

The paper is organized as follows: In the next section, we first described briefly the DT-CWT with advantages in noise study, Section III provides some necessary preliminaries on Bayesian MAP Estimator, as Symmetric Normal Inverse Gaussian (SNIG) processes and presents results on the modeling that indicating their heavy-tailed nature. The design of a Bayesian estimator that exploits the signal. The proposed method and choice of MRI is described in section IV. Section V compares the performance of our proposed algorithm with the performance of current de-noising methods, and quantifies the achieved performance improvement. Finally we conclude.

II. DUAL-TREE COMPLEX WAVELET TRANSFORM (DT-CWT).

Remember that the classical discrete wavelet transform (DWT) provides a means of implementing a multiscale analysis, based on a critically sampled filter bank with perfect reconstruction [14] [15].

However, questions arise regarding the good qualities or properties of the wavelets and the results obtained using these tools, the standard DWT suffers from the following problems described as below:

Shift sensitivity: it has been observed that DWT is seriously disadvantaged by the shift sensitivity that arises from down samples in the DWT implementation [16,17].

Poor directionality: an m-dimension transform (m>1) suffers poor directionality when the transform coefficients reveal only a few feature in the spatial domain.

Absence of phase information: filtering the image with DWT increases its size and adds phase distortions; human visual system is sensitive to phase distortion [18]. Such DWT implementations cannot provide the local phase information.

In other applications, and for certain types of images, it is necessary to think of other, more complex wavelets, who gives a good way, because the complex wavelets filters which can be made to suppress negative frequency components. As we shall see the CWT has improved shift-invariance and directional selectivity [19].

The discrete complex dual tree wavelet transform (DT-CWT) was introduced by N. Kingsburg around in 1990.

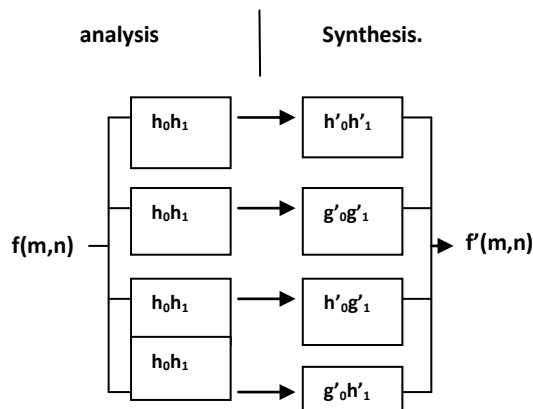
This implementation uses consists in analyzing the signal by two different DWT trees, with filters chosen so that at the end, the signal returns with the approximate decomposition by an analytical wavelet.

The dual-tree structure has an extension of conjugate filtering in 2-D case; this structure is shown in "Fig.1".

This structure needs four trees for analysis as well as for synthesis. The pairs of conjugate filters are applied to two dimensions (0 and 1), which can be expressed as:

$$(h_0 + jg_0)(h_1 + jg_1) = (h_0h_1 - g_0g_1) + j(h_0g_1 + g_0h_1) \tag{1}$$

The synthesis of filters suitable for this structure was performed by several people.



Imaginary trees

Figure.1. Filter bank structure for DT-DWT

The wavelet corresponding to the tree's "imaginary part" is very close to the Hilbert transform of the wavelet corresponding to the tree's "real part" [20].

For J level decomposition, the corresponding details subbands at leven η are denoted :HLη^{real},

$$HLη^{im}, LHη^{real}, LHη^{im}, HHη^{real} and HHη^{im}.$$

Where η = 1,2,...,J.

Because of the existence of two trees, it appears that the second noise coefficients moments from such decomposition can be precisely characterized.

The DT-CWT ensures filtering of the results without distortion and with a good ability for the localization function and the perfect reconstruction (PR) of signal.

In the noise study, as with any redundant frame analysis, when a stationary noise, even if white, is subject to a dual decomposition tree, statistical dependencies appear between coefficients [12,18,19], because of the existence of two trees, it appears that the second noise coefficients moments from such decomposition can be precisely characterized.

We observe a de-correlation between primal and dual coefficients located at the same spatial position and an inter-scale correlation, which allows us to choose between several estimators, taking this phenomenon into account.

If we consider an image degraded by a Gaussian n, white, and centered, additive Gaussian noise with a spectral density, the decomposition coefficients are also affected by that same noise as part of the linearity property [22, 20, and 28].

With this advantage we can choose an appropriate estimator for de-noising and the case of DT-DWT

The mathematical expression for a signal observed at point whose coordinates (x,y) in the image is modeled as follows:

$$g(x,y) = f(x,y) + \epsilon(x,y) \tag{2}$$

With g(x,y), f(x,y) and ε(x,y) are respectively the noise coefficient, the original coefficient, and the

Gaussian independent noise. Our goal is to estimate f from g . To do this, we will use an MPE (Maximum Posterior Estimator) filter [7].

In considering the linearity Property In the noise study, as with any redundant frame analysis, when a stationary noise, even if white, is subject to a dual decomposition tree, statistical dependencies appear between coefficients [26,27].

After applying the DT-CWT on (2), we obtain:

$$g_{\eta}(x, y) = f_{\eta}(x, y) + \varepsilon\eta(x, y) \quad (3),$$

Where, $g_{\eta}(x, y)$, $f_{\eta}(x, y)$ and $\varepsilon\eta(x, y)$ denote (x, y) -th wavelet coefficient at level of a particular detail subband of the DT-CWT of g , f , and ε , respectively and η ($\eta=1, 2, \dots, J$).

III. BAYESIAN MAP ESTIMATOR

It is recognized that parametric Bayesian processing presupposes proper modeling for the prior probability density function (PDF) of the signal.

Bayesian models use prior distributions for parameters, this prior can be multi-level and has distributions can control the model results

In this section we describe the Symmetric Normal Inverse Gaussian (SNIG) distribution and some it proprieties before presenting the model, we refer the reader to a recent work of M. I. H. Bhuiyan et al [13,23]. showed that distributions, a family of heavy-tailed densities, are sufficiently flexible and rich to appropriately mode wavelet coefficients of images in image de-noising applications with better models the prior statistics of the signal components, its probability density function reads as follows [23]:

$$P_f(f) = A \frac{K_1(\alpha\sqrt{\delta^2+f^2})}{\sqrt{\delta^2+f^2}} \quad (4)$$

Where $A = \frac{\alpha \delta \exp(\delta \alpha)}{\pi}$, K_1 denotes the modified Bessel function of second kind with index 1 [24], the parameter α control the shape of the distribution and δ is the a scale parameter. IN additional to illustrate the efficiency of the proposed prior, the generally Gaussian (GG) and SNIG PDFs are fitted to wavelet coefficients of the subbands $HH^{real}1$ for the medical image. Since in DT-CWT, we applied two real DWT, we assure the distribution of the noise coefficients in each DWT is a Gaussian with zero mean and standard deviation σ_{ε}^2 , and denote it by $P_{\varepsilon}(\varepsilon)$.

The Bayesian MAP estimator is given by [8] as follow:

$$\hat{x}(g) = \arg \max P_{\varepsilon}(g - f)P_f(f) \quad (5)$$

To obtain the MAP estimate, the derivative of the logarithm of the in (5) is the st to resulting in:

$$\frac{x-y}{\sigma^2} + p'(f) = 0 \quad (6)$$

Where $p(f) = \ln P_f(f)$ and $p'(f) = \frac{\partial}{\partial f} p(f)$. Using the approach proposed by Hyvarinen [25], an approximate solution of [7] is obtained as:

$$\hat{x}(g) \text{sign}(g) \max(|g| - \sigma_{\eta}^2 |B|, 0) \quad (7) \text{Where}$$

$$B = \frac{2g}{\delta^2+g^2} + \frac{\alpha g}{\sqrt{\delta^2+g^2}} \frac{K_0(\alpha\sqrt{\delta^2+g^2})}{K_1(\alpha\sqrt{\delta^2+g^2})} \quad (8)$$

In this step we need to estimate the parameters α , δ and σ_{η}^2 to obtain the MAP estimates. In order to take noise correction into account for each real DWT tree of the DT-CWT. The corresponding value of σ_{η} is obtained using the coefficients in the corresponding finestsubbands of diagonal orientation as:

$$C = C \frac{D_1+D_2}{2} \quad (9) \text{Where } D_1 = \text{MAD}(g(k,l)) / 0,6745, g(k,l) \in \text{HH1 and}$$

$D_2 = \text{MAD}(g(k,l)) / 0,6745, g(k,l) \in \text{HH2}$, C is a smoothing factor, (MAD is the Median absolute deviation).

To obtain the SNIG parameters for the (k, l) -th coefficient, the estimates of the second and fourth order signal moments denoted by $\widehat{m}_2(k, l)$ and $\widehat{m}_4(k, l)$, respectively, as obtained as:

$$\widehat{m}_2(k, l) = \max((m_2(k, l) - \sigma_{\eta}^2), 0) \quad (10)$$

$$\widehat{m}_4(k, l) = \max((m_4(k, l) - \sigma_{\eta}^2 m_2(k, l) - 3\sigma_{\eta}^4), 0)$$

The values of $m_2(k, l)$ are obtained using a DXD square window as

$$m_2(k, l) = \frac{1}{D^2} \sum_{i=-(M)/2}^{(M)/2} \sum_{j=-(M)/2}^{(M)/2} g(k-i, l-j)^2 \quad (11)$$

$$m_4(k, l) = \frac{1}{D^2} \sum_{i=-(M)/2}^{(M)/2} \sum_{j=-(M)/2}^{(M)/2} g(k-i, l-j)^4$$

Where $M = D-1$. Next, the corresponding second and fourth order cumulants, denoted by \widehat{K}_2 and \widehat{K}_4 respectively, are obtained as:

$$\widehat{K}_2 = \widehat{m}_2$$

$$\widehat{K}_4 = \max((\widehat{m}_4 - 3\widehat{m}_2^2), 0) \quad (12)$$

The parameters α and δ are estimated as

$$\alpha = \sqrt{\frac{3\widehat{K}_2}{\widehat{K}_4}} \delta = \alpha \widehat{K}_2 \quad (13)$$

IV. PROPOSED METHOD

The de-noising diagram involves the following steps shown in diagram "Fig. 2".

- (1) Take the MRI image without contrast agent
- (2) Add noisy into this image (to obtain a noisy MRI image)
- (3) Compute the DT-CWT (dual-tree complex wavelet) of the noisy MRI image,
- (4) Obtain the Bayesian MAP estimator using equation (5)
 - or Compute the threshold value for each pixel for Visu shrink in all sub band details wavelet coefficients [26]
 - or applying Bivariate MAP estimator, in all sub band details wavelet coefficients [27].

- (5) Compute the inverse dual-tree complex (IDT-CWT) using synthesis filter bank forobtained the de-noised image.

where \hat{I} and I denote the noise free and the noised images respectively and N^2 is the total pixels [29].

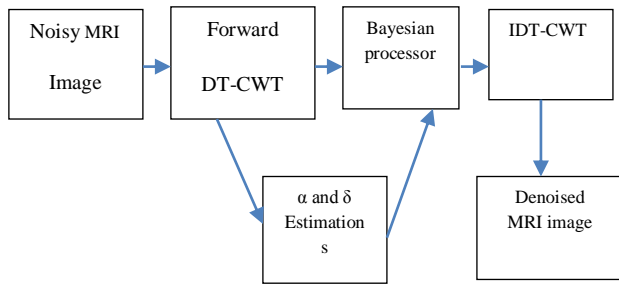


Fig 2. Diagram of proposed de-noising method

Choice of the images

MRI images are diverse and specific. Our study takes into account the behavior of different structures in comparison to contrast agents, because we are convinced that all structures do not react the same way to these agents. Our choice is geared to cranial images, in collaboration with the MRI department of the CHEIK ZHAID International University Hospital, based in Morocco. We selected brain MRI images of two of the four most commonly used sequences, axial and coronal ‘Fig. 3’, for ethical reasons, we decline to identify the patient.

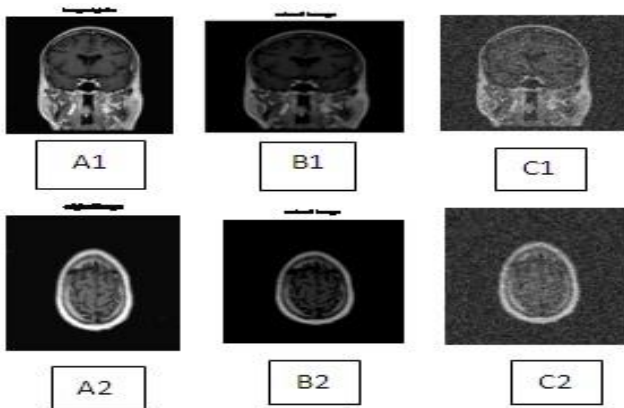


Figure 3.Reference images with contrast agent (A1 and A2.), the same images without contrast (B1 and B2) and noisy images (C1 and C2) respectively.

We compare our proposed algorithm to other effective techniques from the recent literature using MRI images.

From the first category of thresholding, we select the Vusu Shrinkage and Bivariate shrinkage[26], [27], in the second set we used only the adaptive Wiener filter implemented in CWT domain and considered window of size 7x7 within subband.

To quantify the noising performance of each algorithm, we employed the Peak-Signal to-Noise-Ratio (PSNR) defined as

$$PSNR = 20 \log_{10} \left(\frac{256}{\sqrt{\frac{1}{N^2} \sum (\hat{I} - I)^2}} \right) \quad (14)$$

V.Results and Discussion

In the simulations, complex zero mean white Gaussian noise with standard deviation $\sigma \epsilon = 20$, was added to the images without contrast agent (C1 and c2)

The noisy image is decomposed using only the dual tree wavelet transform (DT-CWT), for both the discrete (real DWT) and the complex parts (CWT), because the previous works have sufficiently proved the superiority of DT-CWT over DWT in image de-noising [15,28]

For each decomposition, the number of resolution levels is set in order to obtain equivalent size approximations (as much as possible) at the coarser resolution.

Table 1 give the results obtained the category of thresholding, has, Visu Shrinkage and Bivariate Shrinkage. In Table2, we show results obtained with adaptive Wiener adaptive filter

From the tables it can be seen that our approach achieves the best results in most situations, followed by Bivariate method.

Figure 4 and 5 illustrates the results with the first set of thresholding and Wiener adaptive filter respectively.

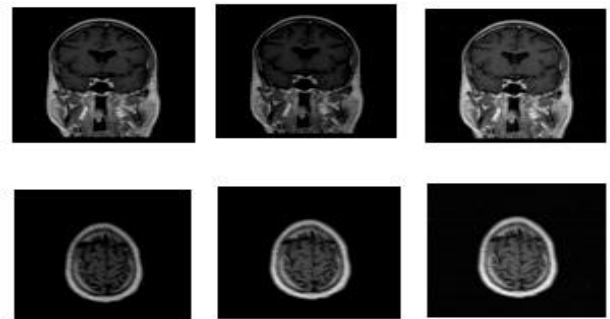


Figure 4. Coronal and Axial images de-noised with Visushrink (left), Bishrink (middle) and proposed method (right) with ($\sigma = 10$)

The PSNRs and Similarity between restored and original image as shown in table1 and2 for each case.

Table 1.PSNR VALUES (dB) OBTAINED BY THE TREE DE-NOISING METHODS

Image	Coronal MRI Image				Axial MRI Image			
	10	15	20	25	10	15	20	25
σ	10	15	20	25	10	15	20	25
Noisy	27.18	23.65	21.14	20.17	28.26	24.55	22.25	20.45
Visushrink	30.76	29.00	28.25	27.44	31.51	30.43	27.92	26.74
Bishrink	32.85	31.00	29.81	28.77	33.77	32.78	30.11	29.43
Proposed method.	33.26	31.22	30.00	29.09	34.75	33.03	31.87	30.01

TABLE 2. PSNR VALUES (dB) OBTAINED BY WIENER FILTER AND PROPOSED METHOD

σ	Axial MRI Image			Coronal MRI Image		
	Noisy	Wiener filter	Proposed Method	Noisy	Wiener filter	Proposed Method
10	28.26	32.51	33.61	27.18	32.34	32.85
15	24.55	30.43	31.63	23.65	30.87	31.90
20	22.55	28.92	30.19	21.14	29.17	30.17
25	20.45	27.74	29.21	20.17	28.10	29.85
30	18.62	26.73	28.51	18.62	26.13	28.87

We observed a decrease of PSNR between the reference images and those subject to de-noising. To assert the difference caused by the use of a contrast agent in the image, the correlation between the two images is lower, as it is to the naked eye. We clearly noticed that some details were quite visible, due to the contrast agent.

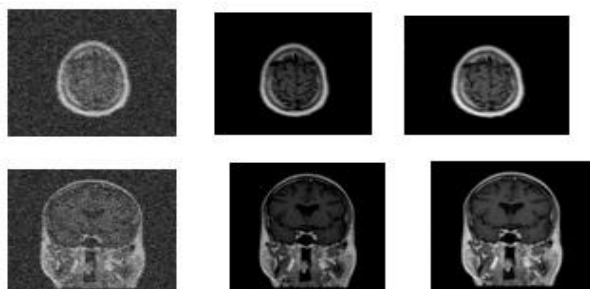


Figure 5. Axial and coronal images de-noised, where noisy images (left), Wiener filter (middle) and proposed method (right) with ($\sigma = 10$)

For the other images with Visu-shrinkage or Bivariate shrinkage (Bishrink), the proposed method shows an even better performance with the Bishrink estimator, where values have improved.

In all cases, the best results were obtained with the proposed method, followed by Bivariate shrinkage with Wiener filter and finally Visu shrinkage, figures and tables shows.

One can also note that the poorer performance was obtained for Visushrink with (increased the value of σ , which remains well below the Bivariate threshold as indicated in Table 1.

Here, we focused particularly on the ability of the our processor structure to de-noise MRI images. In comparison with several existing de-noised methods, the proposed approach out performs results in all cases, the obtained results are provided in Tables 1 and Table 2.

When considering the initial PSNR between original images and degraded images, it shown this approach providing a superior gain for each estimator. We then turned our attention to the test addressed to radiologists on the image quality, also obtaining, in their consideration and as a result of the simulations, a better performance for our processor, compared to other techniques.

The test methodology is detailed below:

Considering the brain images of four sequences commonly used in MRI, axial, coronal, presented to four experienced radiologists working in university hospitals and Sino-congolaise hospital.

In a first stage, the anonymous images were given to the radiologists and they were asked whether the image presented to them was original or restored and if it was acceptable for the diagnosis, to which they could answer yes or no.

Secondly, the restored images compared to the reference images were placed side by side and in this case the original was revealed to the observer, blinded to the type of transform used to restore the image to compare. The radiologists were asked to quantify on a scale of 1 to 9, as follows:

- 9 No visible difference
- 7 No loss of diagnostic information
- 5 In the limit of information loss, discrete anomalies may be omitted.
- 3 Important diagnostic information may be omitted, and the degradation affects the interpretation.
- 1 Unsatisfactory for diagnosis; indisputable loss of diagnostic information.

From this test, we obtained the following observations:

For two of four observers, axial sequence images de-noised with Visu shrink estimator ($\sigma > 20$) were considered non-diagnostic cases.

One observer rejected the coronal sequence images restored with Visushrink estimator ($\sigma > 20$).

Axial images were considered acceptable for diagnosis by all observers for all techniques without Visu shrink estimator ($\sigma > 20$)

In the case where the original or reference image is revealed, we obtained the following results:

Axial: 75% of the observers found no significant loss of diagnostic information for the proposed approach. One observer judged the images de-noised with the Visushrink estimator ($\sigma > 15$) estimator too degraded to be reliable.

Coronal: One observer has considered an image de-noised Visushrinkage at the limit of information loss and marked it as a 5.

Axial: All observers agreed on the absence of significant loss of diagnostic information for proposed method, images with the Bivariate estimator and Wiener filter.

Axial: Three observers classified the images in the 5-6 categories, within the diagnostic information loss limit, for Visu Shrinkage.

VI. CONCLUSION

Given the simulation results obtained with our approach, we can state, as described in the literature, this processor is more efficient than others. Its extension to the complex case has especially proved to be interesting and leads to better results than the discrete case. Moreover, the combination with DT-CWT and different MAP estimator offered encouraging results.

Far from the consideration of matching or competing with the use of contrast agents, our study is meant as a statement, indicating that it is possible, with computer processing and the appropriate estimators, to restore a noisy medical image and to highlight certain pathologies the distinction of healthy and pathological tissue.

This can result in a solution on the social level, taking into account the cost of an MRI exam with contrast agents. Finally, the results of the simulation carried out on selected MRI images has allowed us to ascertain that our approach is very favorably positioned compared to the existing medical image de-noising techniques.

ACKNOWLEDGEMENTS

WE WOULD LIKE TO THANK THE RADIOLOGIST RESPONDENTS IN UCH CHEIKZAID AND SINO-CONGOLAISE HOSPITAL FOR THEIR EXCELLENT SCIENTIFIC CONTRIBUTIONS.

REFERENCES

- [1] W.A. Edelstein, G. Glover, C. Hardy, and R. Redington, "The intrinsic signal-to-noise ratio in NMR imaging," *Magn. Reson. Med.*, vol. 3, pp. 604–618, 1986.
- [2] H. Gudbjartsson and S. Patz, "The Rician distribution of noisy MRI data," *Magn. Reson. Med.*, vol. 34, pp. 910–914, 1995.
- [3] X. Li and M. Orchard, "Spatially adaptive denoising under overcomplete expansion," *Proc. IEEE Internat. Conf. on Image Proc., ICIP00*, Vancouver, Canada, Sep 2000.
- [4] E.R. McVeigh, R.M. Henkelman, and M.J. Bronskill, "Noise and filtration in magnetic resonance imaging," *Med. Phys.*, vol. 3, pp.
- [5] R.D. Nowak, "Wavelet-based Rician noise removal for magnetic resonance imaging," *IEEE Trans. Image Proc.*, vol. 8, pp. 1408–1419, Oct 1999.
- [6] A. Macovski, "Noise in MRI," *Magn. Reson. Med.*, vol. 36, pp. 494–497, 1996.
- [7] Wiem Fourati & Mohamed Salim Bouhlel, "Nouvelle méthode pour le débruitage d'images," *4th International Conference: Sciences of Electronic, Technologies of Information and Telecommunications* March 25-29, 2007 – TUNISIA.
- [8] Achim, A., Bezerianos, A., and Tsakalides, P. (2001). Novel bayesian multiscale method for speckle removal in medical. *IEEE Transactions on Medical Imaging*, 20(8):772-783.
- [9] Junmei Zhong and Ruola Ning, "Image Denoising based on wavelets and Multifractals for singularity detection," *IEEE transaction on image processing*, vol.14, n0.10, october 2005.
- [10] Alexandru SAR, André QUINQUIS and al, "Débruitage des images SAR : Application de la TODDE (Transformée en Ondelettes Discrète à Diversité enrichie)" *IEEE Transactions*, 2003.
- [11] J. Weaver, Y. Xu, D. Healy, and J. Driscoll, "Filtering MRI images in the wavelet transform domain," *Magn. Reson. Med.*, vol. 21, pp. 288–295, 1991.

- [12] Y. Xu, J. B. Weaver, D. M. Healy, J. Lu, "Wavelet transform domain filters: a spatially selective noise filtration technique," *IEEE Trans. Image Proc.*, vol. 3, no. 6, pp. 747–758, Nov. 1994
- [13] M.I.H Bhuiyan, M.Omain Ahmad and al, 'wavelet-based despeckling of medical ultrasound images with the Symmetric Normal Inverse Gaussian prior' 2007 *IEEE, ICASSP* 2007.
- [14] Mallat, 'A wavelet tour of signal processing' San Diego, CA, USA : *Academic Press*, 1998
- [15] RudraPratap Singh Chauhan, Sanjay Singh and al, 'Study and Performance Appraisal of CDWT for Image Quality Improvement and De-noising', *Pragyaan : Journal of Information Technology* Volume 9 : Issue 2, 'December 2011
- [16] N.G Kinsbury. Image processing with complex wavelets'. *Phil. Trans. Royal Society* London, 1999.
- [17] N.G Kinsbury. 'A dual-tree complex wavelet transform with improved orthogonality and symmetry proprieties'. In *Proceedings of the IEEE, Int. Conf. on Image Proc. (ICIP)*, 2000
- [18] H. Guo, 'Theory and applications of shift-invariant, time-varying and undecimated wavelet transform' MS thesis, Rice University, 1995.
- [19] N.G Kinsbury. 'Image processing with complex wavelets'. *Phil. Trans. Royal Society* London, 1999.
- [20] I. Selesnick and K. Li. 'videodenoising using 2D and 3D dual-tree complex wavelet transforms: in wavelet applications in signal and image processing' *X (proc. SPIE 5207)* 2003.
- [21] N.G Kinsbury. 'A dual-tree complex wavelet transform with improved orthogonality and symmetry proprieties'. In *Proceedings of the IEEE, Int. Conf. on Image Proc. (ICIP)*, 2000
- [22] I. Selesnick, R.G. Baraniuk and N.G. Kingsbury, 'The dual-tree complex wavelet transform: *IEE Signal Processing magazine*, vol. 22, n°6, pp. 123–151, nov. 2005.
- [23] M.I.H Bhuiyan, M.Omain Ahmad and al, 'Spatially adaptive wavelet-based method using the Cauchy prior for de-noising the SAR images', *IEEE Trans. on Circuits, Systems and video Thecnology* (in press), 2007.
- [24] A. Hanssen and T. A. Oigard, 'The normal inverse Gaussian distribution for heavy-tailed processes,' in *Proc. IEEE EUEASIP Workshop on Nonlinear Signal and Image processing*, 2001.
- [25] A. Hyvarinen, 'Sparse code shrinkage: Denoising of nonGaussian data by maximum likelihood estimation,' *Neural Computation*, vol. 11, pp. 1739–1768, 1999.
- [26] D L Donoho, 'Denoising by soft thresholding', *IEE Trans. Info, Theory*, 41(3), 613–627, 1995.
- [27] L. Sendur and Ivan Selesnick 'Bivariate Shrinkage function for wavelet-based denoising exploiting interscale dependency', *IEEE Trans. On Signal proc.* 50(11): 2744–2756. (2002).
- [28] RudraPratap Singh Chauhan, Sanjay Singh, Sanjeev Kumar, 'A Practical Approach of Complex Dual Tree DWT for Image Quality Improvement and De-noising' *International Journal of Modern Engineering Research (IJMER)* Vol. 1, Issue.2, pp-632-636
- [29] APPEL W. 'Mathématiques pour la physique et pour les physiciens', *H&K, Paris*, 2002.